1-2012

Template Synthesis of Subnanometer Gold Clusters in Interfacially Cross-Linked Reverse Micelles Mediated by Confined Counterions

Shiyong Zhang
Iowa State University

Yan Zhao
Iowa State University, zhaoy@iastate.edu

Template Synthesis of Subnanometer Gold Clusters in Interfacially Cross-Linked Reverse Micelles Mediated by Confined Counterions

Abstract
A cationic surfactant with a triallylammonium headgroup was cross-linked photochemically in the presence of a hydrophilic dithiol in the reverse micelle (RM) configuration. The interfacially cross-linked reverse micelles (ICRMs) are unusual templates for nanomaterials synthesis. Our previous work indicated that the ICRMs could extract anionic metal salts such as tetracholoroaurate into the hydrophilic interior, and the entrapped aurate was reduced without externally added reducing agent to form subnanometer luminescent gold clusters [Zhang, S.; Zhao, Y. *ACS Nano***2011**, *5*, 2637–2646]. In this work, the bromide counterions were established as the reducing agent in the template synthesis. The reduction of tetrachloroaurate was proposed to happen through ligand exchange on the aurate by the bromide ions, reductive elimination of halogen, and disproportionation of the Au(I) intermediate. The size of the gold clusters could be tuned rationally by the water-to-surfactant ratio ($W0$) and the reducing agent. Monodisperse Au4 and Au9–10 clusters as well as larger Au18 and Au23 clusters were obtained from the ICRM templates. The as-prepared, metastable gold clusters were subject to reconstruction triggered by ligand exchange on the surface but could be stabilized through proper surface protection using a chelating dithiol.

Disciplines
Chemistry

Langmuir

Article

pubs.acs.org/Langmuir

Template Synthesis of Subnanometer Gold Clusters in Interfacially Cross-Linked Reverse Micelles Mediated by Confined Counterions

Shiyong Zhang and Yan Zhao*

Department of Chemistry, Iowa State University, Ames, Iowa 50011-3111, United States

Supporting Information

ABSTRACT: A cationic surfactant with a triallylammonium headgroup was cross-linked photochemically in the presence of a hydrophilic dithiol in the reverse micelle (RM) configuration. The interfacially cross-linked reverse micelles (ICRMs) are unusual templates for nanomaterials synthesis. Our previous work indicated that the ICRMs could extract anionic metal salts such as tetracholoroaurate into the hydrophilic interior, and the entrapped aurate was reduced without externally added reducing agent to form subnanometer luminescent gold clusters [Zhang, S.; Zhao, Y. *ACS Nano* **2011**, *5*, 2637−2646]. In this work, the bromide counterions were established as the reducing agent in the template synthesis. The reduction of tetrachloroaurate was proposed to happen through ligand exchange on the aurate by the bromide ions, reductive elimination of halogen, and disproportionation of the Au(I) intermediate. The size of the gold clusters could be tuned rationally by the water-to-surfactant ratio (W_0) and the reducing agent. Monodisperse Au_4 and Au_{9-10} clusters as well as larger Au_{18} and Au_{23} clusters were obtained from the ICRM templates. The as-prepared, metastable gold clusters were subject to reconstruction triggered by ligand exchange on the surface but could be stabilized through proper surface protection using a chelating dithiol.

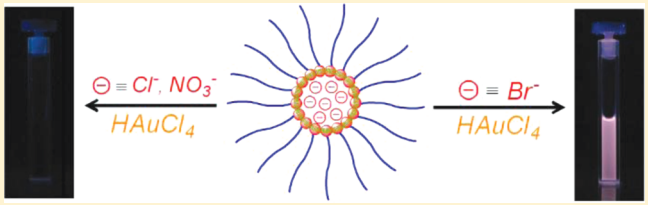

INTRODUCTION

Subnanometer noble metal clusters have attracted the attention of many researchers in recent years.[1,2] As their size approaches the Fermi wavelength (ca. 0.5 nm) of electrons, gold and silver nanoclusters display molecule-like emission. Their size-dependent optical properties, coupled with potentially high photostability, make them promising candidates for optoelectronic applications.[3−12] In addition to their potential applications as bright and nonbleaching molecule-like fluorophores, noble metal clusters are useful catalysts for a range of chemical reactions.[13−16] Since the catalytic activity of a metal catalyst is highly sensitive to its surface property, subnanometer noble metal clusters are very promising catalysts due to their extremely high surface area.[17−21]

The high surface area of subnanometer clusters makes their synthesis particularly challenging. Unless protected by proper passivating ligands, small metal clusters tend to agglomerate into larger particles. In the literature, these ultrasmall metal clusters sometimes were obtained by the fractionation of polydisperse materials.[4,22] Dendrimers are excellent templates for metal nanoclusters due to their monodispersity and well-controlled structures. The template synthesis of subnanometer metal clusters using dendrimers, however, sometimes took days to complete, and postpurification was needed to remove large particles formed as side products.[3,5] An innovative method to produce Au_8 clusters by etching larger nanoparticles with polyethylenimine was reported by Nie et al., but the conversion yield was only about 30%.[6] Other reported templates include proteins,[7] polymer microgels,[9] and star polymers.[10]

We recently reported a facile method to cross-link reverse micelles (RMs) by the thiol−ene click chemistry (Scheme 1).[23] RMs are assemblies of surfactants in nonpolar solvents containing a small amount of water. Although they are widely used as templates for inorganic nanomaterials, their dynamic nature and fast collision make it difficult to control the size and morphology of the final materials.[24,25] In our previous work, a triallylated cationic surfactant (**1**) was cross-linked with a hydrophilic dithiol (dithiothreitol or DTT) under UV irradiation. Covalent capture of RMs in the original size has only been achieved once prior to our work.[26,27] We believe that the high density of the cross-linking functionality (i.e., ene) at the surfactant−water interface, the high efficiency of the thiol−ene reaction, and the water solubility of DTT all contributed to the success. Most interestingly, the resulting interfacially cross-linked reverse-micelles (ICRMs) turned out to be highly unusual templates. The introverted cationic groups easily extracted anionic precursors such as $AuCl_4^-$ and $PtCl_6^{2-}$ into the organic phase. When $NaBH_4$ was employed to reduce the entrapped aurate, nanometer-sized gold particles were obtained unless the aurate loading was kept low. In the absence of externally added reducing agent, the aurate surprisingly underwent "spontaneous reduction" to yield luminescent Au_4, Au_8, and Au_{13}−Au_{23}, depending on the amount of aurate used in the template synthesis.

Received: November 29, 2011
Revised: January 9, 2012
Published: January 20, 2012

Scheme 1. Preparation of ICRM and the Template Synthesis of Subnanometer Gold Clusters

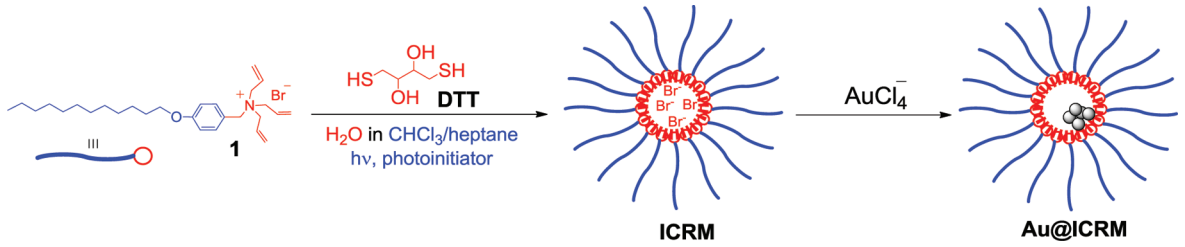

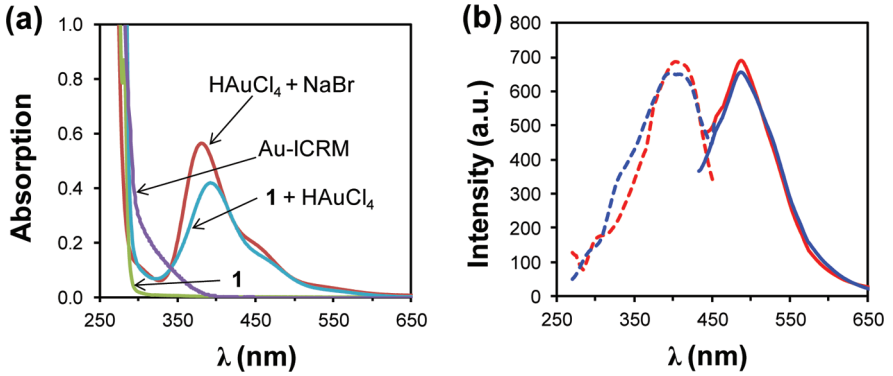

Figure 1. (a) Absorption spectra of aqueous solution of **1** (6×10^{-4} M), a 10:1 mixture of **1** and $HAuCl_4$, a 10:1 mixture of NaBr and $HAuCl_4$, and the Au-ICRM prepared with 10 mol % aurate loading in the absence of externally added reducing agent. $[HAuCl_4] = 1.2 \times 10^{-4}$ M. (b) Emission (solid lines) and excitation (dashed lines) spectra of Au-ICRMs prepared by in situ reduction of aurate by bromide. The red traces are the spectra for the as-prepared samples and the blue traces to those after the addition of N_2H_4 (20 equiv to the amount of Au in the Au-ICRMs). [Cross-linked **1**] = 3×10^{-3} M, [Au in the Au-ICRMs] = 3×10^{-4} M. $W_0 = [H_2O]/[\text{surfactant}] = 5$.

Our previous work suggests that the aurate inside the hydrophilic core of the ICRM has different reduction potential. In the literature, spontaneous reduction of aurate was reported to be assisted by the dehydration of aurate within block copolymer micelles[28] or by encapsulation within dendrimers.[29] Although similar dehydration and encapsulation could have occurred in our system, we were unable to identify the reducing agent in our previous investigation. Herein, we report that it was the bromide ions that reduced the aurate during the template synthesis and the microenvironment of the ICRM core was responsible for the decreased reduction potential. In addition, the size of the gold clusters prepared in our template synthesis could be controlled rationally by the size of the ICRM core, which determines the number of bromide ions available for the reduction. The gold clusters obtained were protected physically and by weak ligands only. Importantly, the clusters could be post-treated with chelating ligands such as DTT, greatly enhancing their stability.

EXPERIMENTAL SECTION

General. All reagents and solvents were of ACS certified grade or higher and were used as received from commercial suppliers. Routine ^1H and ^{13}C NMR spectra were recorded on a Varian VXR-400 and Bruker DRX-400 spectrometer. DLS studies were performed on a PDDLS/Cool Batch 90 T dynamic light scattering detector at 25.0 °C. The intensity data were analyzed with the PRECISION DECONVOLVE program, and the size measurement was based on five replicates. Fluorescence spectra were recorded at ambient temperature on a Varian Cary Eclipse fluorescence spectrophotometer. UV–vis spectra were recorded at ambient temperature on a Cary 50 Bio UV–vis spectrophotometer. Preparation of ICRMs and template synthesis of Au nanoparticles were reported previously.[23]

Typical Preparation of Au-ICRMs without Externally Added Reducing Agents. A 10 mM aqueous solution of $HAuCl_4$ (2 mL) was added to a 10 mM ICRM solution in chloroform (2 mL). The aqueous phase became colorless, and the organic phase turned yellow upon stirring. Upon sitting at room temperature overnight, the organic phase became colorless. The organic phase was separated, washed with water three times, and concentrated by rotary evaporation. The residue could be redissolved in common organic solvents and were stable over a period of several months.

Ion Exchange of the Bromide Ions in the ICRMs. A 2 M aqueous solution of NaCl (2.0 mL) was added to an ICRM solution in chloroform (2.0 mL, [cross-linked **1**] = 20 mM, $W_0 = 5$). The resulting mixture was stirred vigorously overnight and allowed to settle at room temperature. The organic phase was separated, washed with water, and concentrated *in vacuo* to get a white powder, which was used in subsequent studies directly.

RESULTS AND DISCUSSION

Reducing Role of Counterions in the ICRM-Templated Synthesis of Gold Clusters. "Spontaneous" reduction of aurate has been reported for polymers and dendrimers containing ether[29–32] and amide[33] groups, which normally do not reduce aurate. The ICRMs contain ether, hydroxyl, thioether, and bromide ions; all are potential reducing agents. Since the ICRMs and the Au-ICRMs (i.e., gold clusters prepared within and protected by the ICRMs) gave very similar IR spectra, hydroxyl and thioether do not seem to be involved in the reduction.[23]

The aqueous solution of $HAuCl_4$ gave a broad absorption at 290 nm. The peak tails beyond 400 nm, which explains the light yellow color of the aurate solution. When NaBr and $HAuCl_4$ were mixed in a 10:1 ratio, a new peak appeared at 380 nm (Figure 1a, the red spectrum), indicating the formation of $AuBr_4^-$ ($\lambda_{max} \approx 382$ nm). Cationic surfactant **1** was able to transfer aurate from the aqueous phase into chloroform, giving a new peak at 390 nm as well. We attributed this peak to

dx.doi.org/10.1021/la204694c | *Langmuir* 2012, 28, 3606–3613

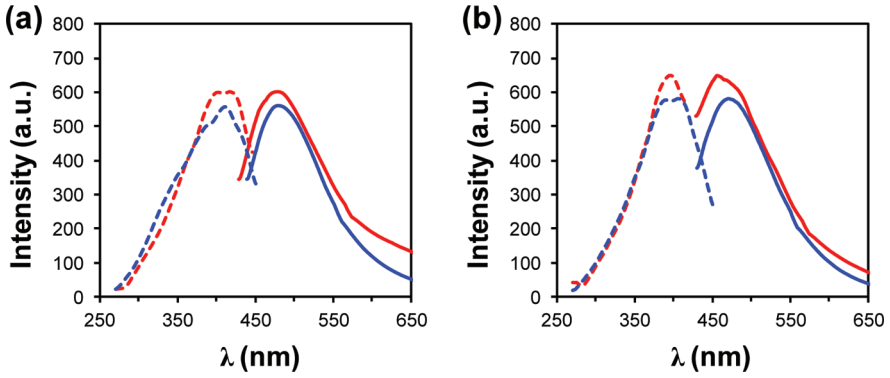

Figure 2. Emission (solid lines) and excitation (dashed lines) spectra of Au-ICRMs prepared by first exchanging the bromide counterions to chloride (a) and nitrate (b), followed by stirring the mixture with an aqueous solution of NaBr (50 equiv to aurate). The red traces correspond to the spectra of the as-prepared samples and the blue traces to those after the addition of N_2H_4 (20 equiv to the amount of Au in the Au-ICRMs). [Cross-linked **1**] = 3×10^{-3} M, [Au in the Au-ICRMs] = 3×10^{-4} M. W_0 = [H_2O]/[surfactant] = 5.

$AuBr_4^-$ formed by the ligand exchange on the aurate by the bromide counterion of **1**. Displacement of the chloride on tetrachloroaurate happens easily, facilitated by both the stronger nucleophilicity and the softness of bromide.[34,35] The 10 nm difference in λ_{max} most likely results from a solvent effect, as the spectrum for the mixture of **1** and $HAuCl_4$ was recorded in chloroform but that for NaBr and $HAuCl_4$ in water.

The ICRMs were also able to transfer the aurate in the aqueous phase to the chloroform phase, but the fate of the aurate was different. Whereas aurate transferred by uncross-linked **1** stayed as $AuBr_4^-$, giving a brown solution, that transferred by the ICRMs faded over time upon entering the organic phase. The absorption spectrum of the chloroform solution in the latter is shown in Figure 1a (the violet spectrum). Note that, although excess bromide was present in our sample ([cross-linked **1**]/[$HAuCl_4$] = 10:1), no peak was observed near 380−390 nm, indicating the absence of $AuBr_4^-$.

The gold clusters were too small to be visualized by techniques such as TEM.[23] The colorless Au-ICRMs emitted pink luminescence under a hand-held UV lamp (λ = 365 nm). Figure 1b shows the emission and excitation spectra of the Au-ICRMs prepared with 10 mol % aurate at W_0 = [H_2O]/[surfactant] = 5. The water-to-surfactant ratio (W_0) controls the size of the water pool in the RMs and also the hydrophilic core size for the ICRMs. The excitation and emission wavelengths were 402 and 487 nm, somewhat higher than the 375 and 451 nm observed previously for similar Au-ICRMs prepared at the same aurate loading but lower W_0.[23] The transition energy of gold clusters are known to scale with the inverse cluster radius.[2] Assuming that the ICRM-encapsulated Au clusters and those protected by PAMAM dendrimers have the same energy−size relationship, the excitation/emission wavelengths of 402/487 nm correspond to Au_9−Au_{10} clusters and 375/451 nm to Au_8.[36] The slight increase of cluster size with W_0 was reasonable. Both the core size of the ICRM and the number of surfactants in the core increase with the water-to-surfactant ratio,[37] so is the number of bromide counterions. The larger Au clusters obtained at higher W_0 suggests that bromide could be the reducing agent involved (vide infra).

Hydrazine (N_2H_4) is a strong reducing agent. Mixing hydrazine and aurate in our hands caused instantaneous formation of black gold precipitate if no passivating ligands were present. As shown by the blue spectra in Figure 1b, the addition of hydrazine (20 equiv to the amount of Au in the Au-ICRMs) produced negligible changes in the excitation and emission spectra. The result corroborated with the disappearance of the $AuBr_4^-$ absorption (Figure 1a) and confirmed that the aurate was reduced after being transferred into the organic phase by the ICRMs.

To further verify the reducing role of the bromide counterion, we replaced the bromide ions of the ICRMs by chloride and nitrate. The ion-exchanged ICRMs were prepared by stirring a chloroform solution of ICRMs with a concentrated, 2 M aqueous solution of sodium chloride and sodium nitrate, respectively. Not surprisingly, when aurate was extracted into the organic phase by the chloride- and nitrate-containing ICRMs, the light yellow color of the aurate stayed and no luminescence was detected for the resulting samples. Most importantly, after the aurate-loaded ICRMs were stirred with an aqueous solution of NaBr, the same luminescence appeared for both ion-exchanged samples (Figure 2), demonstrating unequivocally the importance of bromide ions in the reduction.

As shown by the mixing experiment for NaBr and $HAuCl_4$ (Figure 1a), $AuBr_4^-$ was quite stable in water. Because mixing uncross-linked **1** and $HAuCl_4$ yielded the ligand-exchanged product (i.e., $AuBr_4^-$) instead of gold clusters, the stability of $AuBr_4^-$ must be quite different in the un-cross-linked RMs and in the ICRMs. In the literature, when dehydrated within block copolymer micelles[28] or encapsulated within dendrimers, aurate was reported to be reduced by otherwise unlikely functional groups such as poly(ethylene glycol).[29] Although the ICRM core contains a nanosized water pool, the entrapped aurate is not expected to be fully solvated as in aqueous solution. Quite likely, similar dehydration and encapsulation lowered the reduction potential of the ICRM-encapsulated aurate and promoted the otherwise difficult reaction.

The reduction of tetrahaloaurate takes place in a two-step process.[38,39] The first step involves reductive elimination of X_2 (eq 1), but the resulting AuX_2^- is unstable and disproportionates in the second step to form tetrahaloaurate and reduced gold (eq 2). The net result is shown in eq 3, showing the formation of Au(0) from AuX_4^-, releasing X_2 as the byproduct. The reaction is known to happen extremely readily with iodide.[39,40] Although less frequent, tetrabromoaurate can undergo the same reaction under suitable conditions.[41] For tetrachloaurate, the reaction often needs additional assistance such as UV light.[42] It should be mentioned that the formation of gold clusters within the ICRMs took place in our hands also in darkness, indicating that light was not playing a role in the

dx.doi.org/10.1021/la204694c | *Langmuir* 2012, 28, 3606−3613

reduction. Also note that a complete ligand exchange is not necessary for the aurate reduction. A partially exchanged product, e.g., $AuCl_2Br_2^-$, may very well be able to undergo reductive elimination.

$$AuX_4^- \leftrightarrows AuX_2^- + X_2 \quad (1)$$

$$3AuX_2^- \leftrightarrows AuX_4^- + 2Au(0) + 2X^- \quad (2)$$

$$AuX_4^- \leftrightarrows 2Au(0) + 3X_2 + 2X^- \quad (3)$$

Our previous study showed that different reducing agents produced very different clusters using ICRMs at $W_0 = 1$.[23] The same happened again at $W_0 = 5$. As shown by Figure 3, the

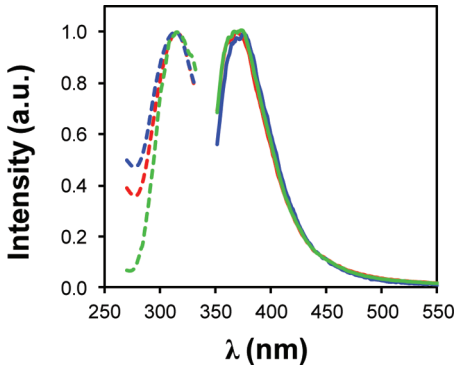

Figure 3. Normalized emission (solid lines) and excitation (dashed lines) spectra of Au-ICRMs prepared by reducing the ICRM-entrapped aurate with $NaBH_4$. The counterion in the ICRMs prior to aurate loading was bromide, chloride, and nitrate for the green, red, and blue spectra, respectively. [Cross-linked **1**] = 3×10^{-3} M, [Au in the Au-ICRMs] = 3×10^{-4} M. W_0 = [H_2O]/[surfactant] = 5.

ICRM-encapsulated aurate, regardless of the counterions present, was reduced by sodium borohydride ($NaBH_4$). Ultrasmall gold clusters were also obtained, but the excitation/emission wavelengths were ~315/370 nm. These numbers match well with those for the Au_4 reported in the literature, 313/371 nm.[5] One likely reason for the different result was the anion adsorption on the gold surface. A particle made of several metal ions has an extremely large surface-to-volume ratio. Different anions have different affinities toward gold surface and, most importantly, anion adsorption is known to cause reconstruction of metal surfaces.[43] For subnanometer gold clusters, such reconstruction is extremely facile because all the gold atoms are on the surface and associated with the surface ligands. The stability of gold clusters is affected by both the intrinsic stability of the gold core and the surface ligands.[4] For halides, the binding affinity follows the order of $F^- < Cl^- < Br^- < I^-$.[44] Bromide adsorption on the gold surface is quite strong and reported to affect the growth of gold nanomaterials.[45−51] Quite likely, Au_9−Au_{10} were the most favorable clusters when the aurate was reduced slowly and protected by bromide ions (or other weak ligands present in the ICRM core). When (excess) borohydride was used as a reducing agent, not only the reduction happened through a different mechanism but also the surface of the gold clusters was probably covered by different ligands. These differences likely were responsible for the formation of the Au_4 clusters in the latter case.

Synthesis of Larger Gold Clusters Using ICRMs with Higher W_0. Our study so far confirmed that the ICRM-confined bromide ions were responsible for the reduction of the aurate. The most likely mechanism was the ligand exchange on tetrachloroaurate followed by reductive elimination and disproportionation of the resulting AuX_2^-. The formation of the gold clusters seemed to be slow, with the fluorescence and absorption spectra becoming stable in several hours after the aurate was transferred into the organic phase. The slow reaction was reasonable given the many cycles of reductive elimination and disproportionation needed before the tetrahaloaurate could be completely reduced.

If bromide is indeed involved in the aurate reduction, three bromide ions are needed to reduce one aurate if the reduction takes place exclusively according to eqs 1−3. In other words, the reduction of the aurate would be limited by the number of bromide ions inside the ICRM, and a maximum of 0.33 equiv of aurate would be reduced under the condition. The hypothesis, if correct, also predicts larger gold clusters would result if more bromide ions are present in the ICRM core during the template synthesis. The 0.33 equiv limit, of course, would not apply if reductive elimination could occur also for Cl_2 or BrCl (see eqs 1−3).

To test these hypotheses, we increased the water-to-surfactant ratio (W_0) to 20. As the size of the water pool increases in the RM, more surfactants would assemble around the water pool, giving more bromide ions in the resulting ICRMs. Figure 4 shows the normalized spectra of Au-ICRMs prepared by extracting 10, 30, 50, 70, and 100 mol % aurate from the aqueous phase into the chloroform phase. The clusters

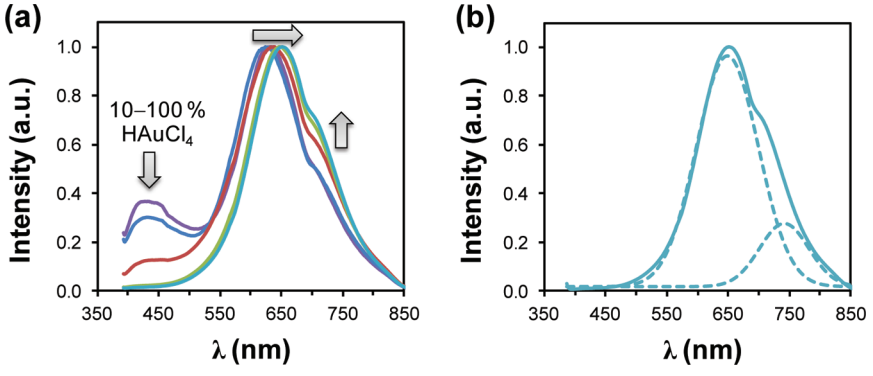

Figure 4. (a) Normalized emission spectra of Au-ICRMs prepared by *in situ* reduction of aurate. The aurate loading in the samples were 10, 30, 50, 70, and 100 mol %. W_0 = [H_2O]/[surfactant] = 20. [Cross-linked **1**] = 3×10^{-3} M. λ_{ex} = 363 nm. (b) Peak-fitting of the spectrum for the Au-ICRM prepared with 100% aurate loading, yielding two peaks centered at 650 and 740 nm, respectively.

dx.doi.org/10.1021/la204694c | *Langmuir* 2012, 28, 3606−3613

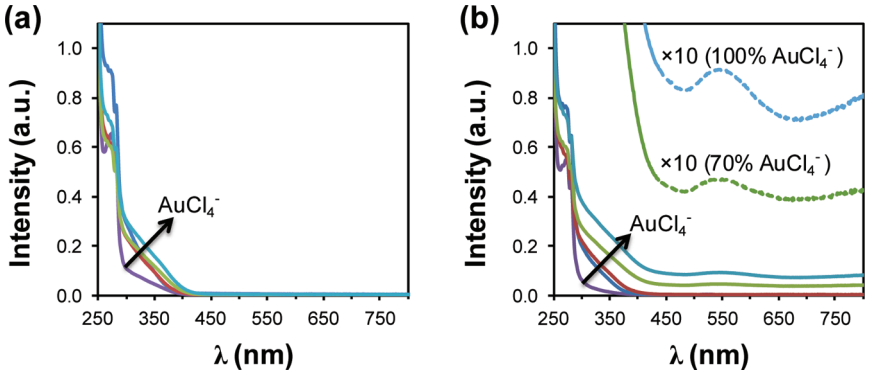

Figure 5. Absorption spectra of Au-ICRMs (a) prepared by *in situ* reduction of aurate by bromide and (b) after the addition of N_2H_4 (20 equiv to amount of Au in the Au-ICRMs). The aurate loading in the samples were 10, 30, 50, 70, and 100 mol % from left to right. [Cross-linked **1**] = 2×10^{-4} M. W_0 = 20.

obtained at W_0 = 20 were distinctively different from those at W_0 = 5, even at the same aurate loading. Instead of a single peak at 480−490 nm, three peaks could be identified for the Au-ICRMs prepared at W_0 = 20 with 10 mol % aurate (Figure 4a). The weak peak at 440−450 nm corresponds to Au_8.[36] The most prominent peak appeared near 630 nm, with another shoulder at 740 nm revealed by peak fitting (Figure 4b). The emission for PAMAM-protected Au_{13} and Au_{23} clusters occur at 511 and 752 nm, respectively. Assuming that the electronic transition was not affected significantly by the different surface ligands, the 640 and 740 nm emission wavelengths should come from Au_{18} and Au_{23} clusters, respectively.[36] As the aurate loading increased further to 100 mol %, the emission from Au_8 disappeared and the peak for Au_{23} at 740 nm increased in intensity. At the same time, the dominant peak near 640 nm shifted to the red, also indicating the formation of larger clusters.

The above results overall were in line with our expectations. An increase of W_0 increases the size of the internal water pool and the aggregation number of the RM. The hydrodynamic diameters of the RM of **1** at W_0 = 5 and 20 were 6.1 and 12.0 nm, respectively, according to DLS (Figures 1S and 2S in the Supporting Information). For the RM of sodium bis(2-ethylhexyl) sulfosuccinate or AOT, a change of W_0 from 5 to 20 increased the aggregation number from ca. 70 to 300 and the size of the water pool from 1.5 to 6 nm.[52,53] Although surfactant **1** is quite different from AOT in structure, the same trend should apply.[54] At the lower W_0, not only the number of bromide ions limits the potential number of aurate ions to be reduced, the physical size of the water pool of the ICRM also restricts the number of the aurate ions that can enter. Because Au_n clusters prefer certain "magic" numbers,[4] the clusters formed at the lower W_0 probably represent the most stable ones allowed under the these constraints. At the higher W_0, however, both constraints (i.e., the available reducing agent and the physical size of the ICRM core) become less important. Because more aurate ions are allowed to enter the ICRM core, larger (and yet stable) clusters could form potentially. The polydispersity of the clusters most likely results from the different numbers of aurate ions that have entered the different ICRMs.

A question remains on whether all the aurate was reduced, especially for the samples with high aurate loading. To understand the completeness of the reduction, we treated the samples with excess hydrazine. If any unreduced aurate was present, hydrazine is expected to reduce it quickly. Depending on where the aurate was located, the reduced gold could either stay inside the ICRM core and be protected or precipitate out of the solution if no appropriate passivating ligands are present.

Addition of hydrazine in general did not change the emission wavelength of the Au-ICRMs prepared at the different levels of aurate loading. Although a decrease in emission intensity was observed, the effect could be caused by inadvertent quenching or the change of surface property of the gold clusters. The absorption spectra, on the other hand, provided more clues to the status of the aurate extracted by the ICRMs.[55] Figure 5a shows the UV−vis spectra of the as-prepared Au-ICRMs after aurate extraction. For all five samples, the peak for $AuBr_4^-$ (λ_{max} = 390 nm and absorption beyond 450 nm, see Figure 1a) was absent. Although the data were consistent with the reduction of the aurate, the same result would also be obtained if not all the tetrachloroautate underwent ligand exchange (and reduction). Because $AuCl_4^-$ absorbs at 290 nm, the peak could easily be obscured by the absorption of Au-ICRMs. We consider the latter explanation more reasonable, as there were not enough bromide ions in the ICRMs to reduce all the aurate according to eqs 1−3. Indeed, after the addition of 20 equiv of hydrazine, although the spectra for the Au-ICRMs prepared with 10−50 mol % aurate were unaffected, those with 70 and 100% aurate changed significantly (Figure 5b). For the latter samples, not only the absorption across the entire UV−vis region became higher, a weak but notable peak appeared near 550 nm, indicating the formation of much larger nanoparticles.[56]

The above observations are quite consistent with the aurate reduction mechanisms described in eqs 1−3.[57] We are not absolutely certain that only 0.33 equiv of aurate was reduced by the ICRM-confined bromide ions because the sample prepared with 50 mol % aurate did not display noticeable changes in the absorption spectrum. It is possible that the sensitivity of this experiment was not enough to detect the small amount of unreduced aurate present in the sample. Alternatively, a small degree of reduction could have occurred via reduction elimination of BrCl—a possibility that could not be completely eliminated by our data.

Because tetrachloroaurate is much larger than bromide in size, it is unlikely for the ICRM core to physically contain 1 equiv of aurate (especially at low W_0). Of course, once the aurate was reduced, Au(0) takes much less space and more aurate could enter the ICRM core. For the high aurate-loaded ICRMs, the unreduced aurate may not be located inside the ICRM core but loosely associated with the weak ligands (thioether and hydroxyl) near the ICRM core. This is a possible

dx.doi.org/10.1021/la204694c | *Langmuir* 2012, 28, 3606−3613

explanation for the formation of the nanometer-sized gold particles when high aurate-loaded ICRMs were treated with hydrazine (Figure 5b).

Stabilization of ICRM-Encapsulated Au Clusters. The above results suggest that the best way to make gold clusters with the ICRM template is to keep the initial aurate loading relatively low, ≤50 mol %. In this way, most aurate not only can undergo smooth *in situ* reduction but also do so inside the ICRM core. Formation of larger nanoparticles can be thus avoided, and the gold clusters formed would be protected within the hydrophilic core. Because the ICRMs only contain weak ligands such as thioether, hydroxyl, and bromide in the core, the gold clusters obtained from the template synthesis should be metastable. Although metastability may be undesirable in optical applications, surface protection by weak ligands is advantageous for potential applications in catalysis.

The metastability of the clusters became apparent when the as-prepared Au-ICRMs were treated with other reagents. Although 20 equiv of hydrazine did not change the emissive property of the Au-ICRMs significantly (Figure 3S), the same amount of $NaBH_4$ completely destroyed the Au_8 (λ_{em} = 450 nm) and Au_{18} clusters (λ_{em} = 630 nm) and only left behind Au_{23} clusters (λ_{em} = 750 nm).[36] The absorption spectra supported the same conclusion.

We were not surprised by the effect of sodium borohydride on the gold clusters. Anion-induced reconstruction of gold surfaces is a well-established phenomenon.[43] A large excess of borohydride anions could displace the weak ligands (bromide or thioether, for example) on the surface of the gold clusters, altering their stability.[4] If the gold clusters become unstable after the ligand exchange, they could easily migrate out of the ICRM core and agglomerate to form larger nanoparticles or even bulk gold.

Our previous study showed that the ICRM-templated synthesis with $NaBH_4$ as the reducing agent produced both Au_4 clusters and particles several nanometers in size at 10% aurate loading.[23] The larger particles most likely came from the agglomeration of small clusters, similar to what happened in the post-treatment of gold clusters with $NaBH_4$. Without proper surface passivation, agglomeration of gold clusters should occur readily, whether the clusters are formed by direction reduction of aurate or rendered unstable by ligand exchange on the surface. It should be noted that gold migration and agglomeration are norm rather than exceptions whenever the metal surface is not properly protected.[56]

If the above rationale for the disappearance of the Au_4 and Au_{18} clusters is correct, protecting the gold clusters with proper passivating ligands should eliminate the $NaBH_4$-triggered reorganization. In one attempt, we stirred a chloroform solution of Au-ICRMs with an excess of 2,2′-dithiodiacetate ($^-OOC-CH_2S-SCH_2-OOC^-$) aqueous solution. The expectation was that the disulfide anions would replace the chloride and/or bromide ions in the ICRM core and stabilize the gold clusters by the sulfur−gold complexation. Unfortunately, very similar results were obtained when the sample was treated with $NaBH_4$ (Figure 4S), suggesting the treatment was inadequate. Apparently, although sufficient for protecting nanometer-sized gold particles,[58−61] the sulfur−gold bond from the disulfide anion was not enough to stabilize the ultrasmall gold clusters.

After the disulfide ligand failed, we added the hydrophilic chelating thiol, DTT, to the Au-ICRMs. To our gratification, the gold clusters became highly stable. Other than some decrease in emission intensity, the hydrazine- and $NaBH_4$-treated Au-ICRMs showed nearly identical emission and absorption spectra as those from the as-prepared sample (Figure 5S). All the peaks at 450, 640, and 750 nm stayed intact, and no surface plasmon absorption could be detected, showing the absence of larger particles.

The effectiveness of DTT protection could be observed visibly. The top panels of Figure 6 show the photographs of the chloroform solutions of the as-prepared Au-ICRMs and those protected by 2,2′-dithiodiacetate and DTT, respectively (Figure 6a). Addition of an aqueous $NaBH_4$ solution turned the as-prepared Au-ICRMs and 2,2′-dithiodiacetate-protected Au-ICRMs from colorless to brown. The brown color was characteristic of larger gold nanoparticles.[56] As seen in Figure 6b, the DTT-stabilized Au-ICRMs remained colorless after the same treatment. Under a hand-held UV lamp, all three samples emitted orange light before the $NaBH_4$ treatment (Figure 6c). As soon as $NaBH_4$ was added, the unprotected and 2,2′-dithiodiacetate-protected gold clusters lost all the luminescence, whereas the DTT-protected ones was unaffected (Figure 6d).

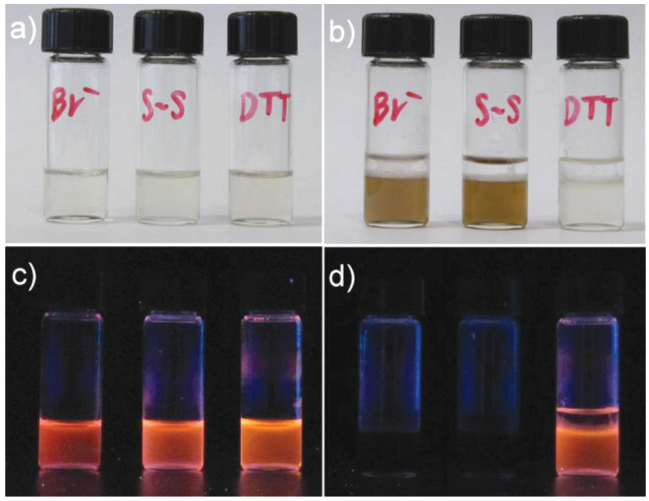

Figure 6. Photographs of Au-ICRMs with the gold clusters protected by bromide, 2,2′-dithiodiacetate, and DTT. The pictures were taken before (a, c) and after (b, d) the addition of aqueous $NaBH_4$ to the chloroform solutions of Au-ICRMs. The bottom pictures (c, d) were taken in the dark under a hand-held UV lamp (λ = 365 nm).

■ CONCLUSIONS

The ICRMs are unique templates for the synthesis of ultrasmall, subnanometer metal clusters. Our previous work showed successful formation of subnanometer gold and gold−platinum nanoclusters.[23] The current study demonstrates unequivocally the reducing role of the confined bromide ions. The hydrophilic core size of the ICRMs determines the number of bromide ions present in a cross-linked reverse micelle and, in turn, controls the possible number of aurate ions to be reduced in the template synthesis. The two-step reductive elimination−disproportionation mechanism makes it straightforward to control the template synthesis. The size of the gold clusters could be tuned by the water-to-surfactant ratio (W_0), the aurate loading, and the reducing agent. Monodisperse Au_4 (Figure 3) and Au_{9-10} clusters (Figures 1b and 2) were obtained for the same ICRM template using different reducing agents. Larger Au_{18} and Au_{23} clusters were obtained with the ICRM templates at W_0 = 20.

dx.doi.org/10.1021/la204694c | *Langmuir* 2012, 28, 3606−3613

The stability of conventional gold nanoparticles derives from surface passivation.[58−61] In our synthesis, the gold clusters were protected physically and by weak ligands such as thiolether and bromide. Notably, our synthesis enabled the formation of both metastable and highly stable gold clusters, depending on the passivating ligands employed. Overall, the straightforward preparation of the ICRM template, the simplicity of the template synthesis, the tunable size and stability of the resulting clusters, and many potential applications of the noble metal clusters make the ICRMs unique templates in nanomaterials synthesis.

■ ASSOCIATED CONTENT

Supporting Information

DLS and additional fluorescence and UV spectra. This material is available free of charge via the Internet at http://pubs.acs.org.

■ AUTHOR INFORMATION

Corresponding Author

*Phone 515-294-5845; Fax: 515-294-0105; e-mail zhaoy@iastate.edu.

■ ACKNOWLEDGMENTS

We thank the U.S. Department of Energy, Office of Basic Energy Sciences (Grant DE-SC0002142), for supporting the research.

■ REFERENCES

(1) Lee, T.-H.; Gonzalez, J. I.; Zheng, J.; Dickson, R. M. *Acc. Chem. Res.* **2004**, *38*, 534−541.
(2) Zheng, J.; Nicovich, P. R.; Dickson, R. M. *Annu. Rev. Phys. Chem.* **2007**, *58*, 409−431.
(3) Zheng, J.; Petty, J. T.; Dickson, R. M. *J. Am. Chem. Soc.* **2003**, *125*, 7780−7781.
(4) Negishi, Y.; Takasugi, Y.; Sato, S.; Yao, H.; Kimura, K.; Tsukuda, T. *J. Am. Chem. Soc.* **2004**, *126*, 6518−6519.
(5) Tran, M. L.; Zvyagin, A. V.; Plakhotnik, T. *Chem. Commun.* **2006**, 2400−2401.
(6) Duan, H.; Nie, S. *J. Am. Chem. Soc.* **2007**, *129*, 2412−2413.
(7) Xie, J.; Zheng, Y.; Ying, J. Y. *J. Am. Chem. Soc.* **2009**, *131*, 888−889.
(8) Zheng, J.; Dickson, R. M. *J. Am. Chem. Soc.* **2002**, *124*, 13982−13983.
(9) Zhang, J. G.; Xu, S. Q.; Kumacheva, E. *Adv. Mater.* **2005**, *17*, 2336−2340.
(10) Shen, Z.; Duan, H. W.; Frey, H. *Adv. Mater.* **2007**, *19*, 349−352.
(11) Zheng, J.; Ding, Y.; Tian, B. Z.; Wang, Z. L.; Zhuang, X. W. *J. Am. Chem. Soc.* **2008**, *130*, 10472−10473.
(12) Maretti, L.; Billone, P. S.; Liu, Y.; Scaiano, J. C. *J. Am. Chem. Soc.* **2009**, *131*, 13972−13980.
(13) Astruc, D. *Nanoparticles and Catalysis*; Wiley-VCH: Weinheim, Germany, 2008.
(14) Bell, A. T. *Science* **2003**, *299*, 1688−1691.
(15) Somorjai, G. A.; Contreras, A. M.; Montano, M.; Rioux, R. M. *Proc. Natl. Acad. Sci. U. S. A.* **2006**, *103*, 10577−10583.
(16) Burda, C.; Chen, X.; Narayanan, R.; El-Sayed, M. A. *Chem. Rev.* **2005**, *105*, 1025−1102.
(17) Lee, H.; Habas, S. E.; Kweskin, S.; Butcher, D.; Somorjai, G. A.; Yang, P. *Angew. Chem., Int. Ed.* **2006**, *45*, 7824−7828.
(18) Narayanan, R.; El-Sayed, M. A. *J. Am. Chem. Soc.* **2003**, *125*, 8340−8347.
(19) Tian, N.; Zhou, Z. Y.; Sun, S. G.; Ding, Y.; Wang, Z. L. *Science* **2007**, *316*, 732−735.
(20) Wang, C.; Daimon, H.; Lee, Y.; Kim, J.; Sun, S. *J. Am. Chem. Soc.* **2007**, *129*, 6974−6975.
(21) Tsung, C. K.; Kuhn, J. N.; Huang, W.; Aliaga, C.; Hung, L. I.; Somorjai, G. A.; Yang, P. *J. Am. Chem. Soc.* **2009**, *131*, 5816−5822.
(22) Schaaff, T. G.; Knight, G.; Shafigullin, M. N.; Borkman, R. F.; Whetten, R. L. *J. Phys. Chem. B* **1998**, *102*, 10643−10646.
(23) Zhang, S.; Zhao, Y. *ACS Nano* **2011**, *5*, 2637−2646.
(24) Pileni, M. P. *Langmuir* **1997**, *13*, 3266−3276.
(25) Pileni, M. P. *Nature Mater.* **2003**, *2*, 145−150.
(26) Jung, H. M.; Price, K. E.; McQuade, D. T. *J. Am. Chem. Soc.* **2003**, *125*, 5351−5355.
(27) Price, K. E.; McQuade, D. T. *Chem. Commun.* **2005**, 1714−1716.
(28) Khullar, P.; Mahal, A.; Singh, V.; Banipal, T. S.; Kaur, G.; Bakshi, M. S. *Langmuir* **2010**, *26*, 11363−11371.
(29) Boisselier, E.; Diallo, A. K.; Salmon, L.; Ornelas, C.; Ruiz, J.; Astruc, D. *J. Am. Chem. Soc.* **2010**, *132*, 2729−2742.
(30) Longenberger, L.; Mills, G. *J. Phys. Chem.* **1995**, *99*, 475−478.
(31) Sakai, T.; Alexandridis, P. *J. Phys. Chem. B* **2005**, *109*, 7766−7777.
(32) Sakai, T.; Alexandridis, P. *Langmuir* **2004**, *20*, 8426−8430.
(33) Hoppe, C. E.; Lazzari, M.; Pardinas-Blanco, I.; Lopez-Quintela, M. A. *Langmuir* **2006**, *22*, 7027−7034.
(34) Cattalin., L.; Orio, A.; Nicolini, M. *J. Am. Chem. Soc.* **1966**, *88*, 5734.
(35) Cattalin., L.; Orio, A.; Tobe, M. L. *J. Am. Chem. Soc.* **1967**, *89*, 3130.
(36) Zheng, J.; Zhang, C.; Dickson, R. M. *Phys. Rev. Lett.* **2004**, *93*, 077402.
(37) Pileni, M. P. *Structure and Reactivity in Reverse Micelles*; Elsevier: Amsterdam, 1989; p xviii, 379 pp.
(38) Elding, L. I.; Skibsted, L. H. *Inorg. Chem.* **1986**, *25*, 4084−4087.
(39) Elding, L. I.; Olsson, L. F. *Inorg. Chem.* **1982**, *21*, 779−784.
(40) Das, A. K.; Raj, C. R. *J. Phys. Chem. C* **2011**, *115*, 21041−21046.
(41) Ettorre, R. *J. Chem. Soc., Dalton Trans.* **1983**, 2329−2332.
(42) Eustis, S.; Hsu, H.-Y.; El-Sayed, M. A. *J. Phys. Chem. B* **2005**, *109*, 4811−4815.
(43) Magnussen, O. M. *Chem. Rev.* **2002**, *102*, 679−725.
(44) Habib, M. A. In *Comprehensive Treatise of Electrochemistry*; Bockris, J. O. M., Conway, B. E., Yeager, E., Eds.; Plenum Press: New York, 1980; Vol. *1*, pp 135−220.
(45) Nikoobakht, B.; El-Sayed, M. A. *Langmuir* **2001**, *17*, 6368−6374.
(46) Gao, J.; Bender, C. M.; Murphy, C. J. *Langmuir* **2003**, *19*, 9065−9070.
(47) Sau, T. K.; Murphy, C. J. *Langmuir* **2005**, *21*, 2923−2929.
(48) Murphy, C. J.; Sau, T. K.; Gole, A. M.; Orendorff, C. J.; Gao, J.; Gou, L.; Hunyadi, S. E.; Li, T. *J. Phys. Chem. B* **2005**, *109*, 13857−13870.
(49) Pérez-Juste, J.; Pastoriza-Santos, I.; Liz-Marzán, L. M.; Mulvaney, P. *Coord. Chem. Rev.* **2005**, *249*, 1870−1901.
(50) Kawasaki, H.; Nishimura, K.; Arakawa, R. *J. Phys. Chem. C* **2007**, *111*, 2683−2690.
(51) Garg, N.; Scholl, C.; Mohanty, A.; Jin, R. C. *Langmuir* **2010**, *26*, 10271−10276.
(52) Day, R. A.; Robinson, B. H.; Clarke, J. H. R.; Doherty, J. V. *J. Chem. Soc., Faraday Trans. 1* **1979**, *75*, 132−139.
(53) North, A. N.; Dore, J. C.; Mcdonald, J. A.; Robinson, B. H.; Heenan, R. K.; Howe, A. M. *Colloids Surf.* **1986**, *19*, 21−29.
(54) Because the ICRM of **1** aggregates in a solvent-dependent fashion, its DLS size cannot be used to estimate the aggregation number. The aggregation was shown not to affect the template synthesis in our previous work. For details, see: Zhang, S.; Zhao, Y. *ACS Nano* **2011**, *5*, 2637−2646.
(55) We previously attributed the unaffected emission wavelength of Au-ICRMs upon hydrazine addition to the complete reduction of aurate (ref 23). From the current work, a more reasonable explanation is that both (reduced) gold clusters and (unreduced) aurate could be present. The already reduced gold clusters were not affected by the hydrazine (10−20 equiv to gold). The unreduced aurate, especially when located outside the ICRM core, aggregated after reduction by

hydrazine and formed larger gold nanoparticles. These larger gold nanoparticles were not luminescent and thus would not affect the emission properties of the small gold clusters within the ICRMs.
(56) Daniel, M. C.; Astruc, D. *Chem. Rev.* **2004**, *104*, 293−346.
(57) To verify the conclusion, we also treated the Au-ICRMs samples (with aurate loading of 10−100 mol %) with excess of aqueous NaBr or UV irradiation; both conditions were known to reduce aurate inside the ICRMs. Although the emission wavelength did not change, black precipitate (bulk gold) was observed for the high aurate samples, most notably for the one with 100 mol % aurate.
(58) Hostetler, M. J.; Wingate, J. E.; Zhong, C. J.; Harris, J. E.; Vachet, R. W.; Clark, M. R.; Londono, J. D.; Green, S. J.; Stokes, J. J.; Wignall, G. D.; Glish, G. L.; Porter, M. D.; Evans, N. D.; Murray, R. W. *Langmuir* **1998**, *14*, 17−30.
(59) Alvarez, M. M.; Khoury, J. T.; Schaaff, T. G.; Shafigullin, M. N.; Vezmar, I.; Whetten, R. L. *J. Phys. Chem. B* **1997**, *101*, 3706−3712.
(60) Schaaff, T. G.; Shafigullin, M. N.; Khoury, J. T.; Vezmar, I.; Whetten, R. L.; Cullen, W. G.; First, P. N.; GutierrezWing, C.; Ascensio, J.; JoseYacaman, M. J. *J. Phys. Chem. B* **1997**, *101*, 7885−7891.
(61) Brust, M.; Fink, J.; Bethell, D.; Schiffrin, D. J.; Kiely, C. *J. Chem. Soc., Chem. Commun.* **1995**, 1655−1656.